Int. J. Heat Mass Transfer. Vol. 36, No. 2, pp. 479–487, 1993
Printed in Great Britain

0017-9310/93 $6.00 + 0.00

Natural convection on vertical and horizontal plates with vectored surface mass transfer

T. S. CHEN, W. P. BUCHANAN and B. F. ARMALY
Department of Mechanical and Aerospace Engineering and Engineering Mechanics, University of Missouri-Rolla, Rolla, MO 65401, U.S.A.

(*Received* 31 *July* 1991 *and in final form* 22 *January* 1992)

Abstract—An analysis is performed to study the flow and heat transfer characteristics of laminar free convection on isothermal vertical and horizontal flat plates with uniform vectored surface mass transfer. The governing equations are first cast into a dimensionless form by a nonsimilar transformation and the resulting equations are then solved by a finite difference method. Numerical results for gases with a Prandtl number of 0.7 are presented for representative values of the normal and streamwise components of the uniform surface mass transfer. For both vertical and horizontal plates, it has been found that an increase in the normal injection ($v_w > 0$) results in a decrease in the local surface heat transfer rate for both downstream vectoring ($u_w > 0$) and upstream vectoring ($u_w < 0$). On the other hand, an increase in the normal suction ($v_w < 0$) results in an increase in the local surface heat transfer rate. For a given value of the normal injection or suction parameter, an increase in the downstream vectoring increases the local surface heat transfer rate and decreases the local wall shear stress. The opposite is true for the case of increasing upstream vectoring. No experimental data are available for comparison.

INTRODUCTION

THIS PAPER is concerned with natural convection in laminar boundary layer flows along vertical and horizontal flat plates with uniform wall temperature and uniform vectored surface mass transfer. Earlier investigations by Swean and Inger [1] and by Chen and Sparrow [2] with vectored mass transfer were confined to forced convection. In the analysis of Swean and Inger, the surface mass transfer comprised of a streamwise component u_w, which was uniform, and a normal component v_w, which varied as $v_w \propto x^{-1/2}$ so that the boundary layer would admit similarity solutions. On the other hand, Chen and Sparrow provided results for both uniform u_w and uniform v_w by introducing a nonsimilarity parameter. More recently, studies on mixed convection with mass transfer have been conducted by Tsuruno and Iguchi [3], Yucel [4], and Dey [5]. Tsuruno and Iguchi studied mixed convection with uniform normal blowing over a vertical plate. The mass transfer parameter was defined as a function of v_w, Re_x, and Gr_x. Yucel's study dealt with mixed convection on horizontal plates with uniform normal mass transfer by combining the buoyancy parameter and the mass transfer parameter to form a nonsimilarity parameter. Dey examined the effect of vectored surface mass transfer in mixed convection over horizontal flat plates. The normal component of the mass transfer v_w was varied as $v_w \propto x^{-1/2}$ so that it led to the similarity solution.

The case of natural convection with mass transfer has received considerably less attention. Parikh *et al.* [6] studied natural convection over vertical plates with variable normal mass transfer, $v_w \propto x^{-1/4}$. The present study treats the effect of uniform vectored surface mass transfer on natural convection over vertical and horizontal flat plates. The results of this analysis should be of general interest in practical problems involving film cooling, control of boundary layers, etc. The conservation equations are converted into a dimensionless form by a nonsimilarity transformation and the transformed equations are then solved by a finite difference method. Numerical results are presented for a Prandtl number of 0.7 and cover a wide range of values of the vectored mass transfer parameters. The effect of downstream vectoring mass transfer ($u_w > 0$ and $v_w > 0$ or $v_w < 0$) and upstream vectoring mass transfer ($u_w < 0$ and $v_w > 0$ or $v_w < 0$) on the flow and thermal fields is discussed.

ANALYSIS

Consider semi-infinite vertical and horizontal flat plates that are situated in a quiescent fluid at an ambient temperature T_∞. The plate is maintained at a uniform wall temperature T_w. The x-coordinate is measured from the leading edge of the plate and the y-coordinate is measured normal to the plate. In the analysis, the vectored surface mass transfer is assumed constant, with a normal component v_w and a streamwise component u_w. The gravitational acceleration g is acting downward. For injection v_w is positive, whereas for suction v_w is negative. The downstream vectoring corresponds to $u_w > 0$ and the upstream vectoring to $u_w < 0$.

In the analysis, the fluid properties are assumed constant except for changes in density that induce the buoyancy force. By using this assumption and applying the Boussinesq approximation, one can write

NOMENCLATURE

f, f_1	reduced stream functions
g	gravitational acceleration
Gr_x	local Grashof number, $g\beta(T_w - T_\infty)x^3/\nu^2$
h	local heat transfer coefficient, $q_w/(T_w - T_\infty)$
k	thermal conductivity
Nu_x	local Nusselt number, hx/k
Pr	Prandtl number, ν/α
q_w	local surface heat flux
T	fluid temperature
u	streamwise velocity component
U_w	dimensionless streamwise component of mass transfer, $(u_w/v_w)/(v_w x/\nu)$
v	normal velocity component
x	streamwise coordinate
y	normal coordinate.

Greek symbols

α	thermal diffusivity
β	volumetric coefficient of thermal expansion
η, η_1	pseudo-similarity variables
θ, θ_1	dimensionless temperatures
μ	dynamic viscosity
ν	kinematic viscosity
ξ, ξ_1	nonsimilar parameters
ρ	density of fluid
τ	local shear stress
ψ	stream function.

Subscripts

w	condition at the wall
∞	condition at the free stream.

the governing equations for laminar boundary layer flow along an inclined plate as [7]

$$\frac{\partial u}{\partial x} + \frac{\partial v}{\partial y} = 0 \tag{1}$$

$$u\frac{\partial u}{\partial x} + v\frac{\partial u}{\partial y} = g\beta\cos\phi(T - T_\infty) + g\beta\sin\phi\frac{\partial}{\partial x}\int_y^\infty (T - T_\infty)\,dy + \nu\frac{\partial^2 u}{\partial y^2} \tag{2}$$

$$u\frac{\partial u}{\partial x} + v\frac{\partial u}{\partial y} = \alpha\frac{\partial^2 T}{\partial y^2} \tag{3}$$

where ϕ is the angle of inclination from the vertical. In the above equations, u and v stand for velocity components in the x and y directions, T is the fluid temperature, β is the volumetric coefficient of thermal expansion, and ρ, ν, and α are the density, kinematic viscosity, and thermal diffusivity of the fluid. The first two terms on the right-hand side of equation (2) represent, respectively, the streamwise component of the buoyancy force and the buoyancy-induced streamwise pressure gradient. For a vertical plate, $\phi = 0$, the second term on the right-hand side of equation (2) disappears. For a horizontal plate, $\phi = \pi/2$, the first term on the right-hand side of equation (2) vanishes. The boundary conditions for this problem are

$$u = u_w, \quad v = v_w, \quad T = T_w \quad \text{at} \quad y = 0$$
$$u \to 0, \quad T \to T_\infty \quad \text{as} \quad y \to \infty. \tag{4}$$

The system of equations (1)–(4) will next be transformed into a dimensionless form. Owing to the constant mass transfer at the wall, the boundary layers are nonsimilar. The transformation will be carried out separately for vertical and horizontal plates.

Vertical plates

For this case, $\phi = 0$, one introduces the dimensionless variables

$$\xi = \xi(x), \quad \eta = \frac{y}{x}(Gr_x/4)^{1/4} \tag{5}$$

where ξ, depending only on x, is the nonsimilar parameter and η is a pseudo-similarity variable. For $\xi(x) = 0$, the boundary layer becomes similar and η becomes a true similarity variable. One also introduces the reduced stream function $f(\xi, \eta)$ and the dimensionless temperature function $\theta(\xi, \eta)$ defined, respectively, by

$$f(\xi, \eta) = \frac{\psi(x, y)}{4\nu(Gr_x/4)^{1/4}}, \quad \theta(\xi, \eta) = \frac{T - T_\infty}{T_w - T_\infty} \tag{6}$$

where $Gr_x = g\beta(T_w - T_\infty)x^3/\nu^2$ is the local Grashof number and $\psi(\xi, \eta)$ is the stream function that satisfies the continuity equation (1) with $u = \partial\psi/\partial y$ and $v = -\partial\psi/\partial x$.

Substituting equations (5) and (6) into equations (1)–(4) with $\phi = 0°$, one obtains the following system of equations:

$$f''' + 3ff'' - 2f'^2 + \theta = \xi\left(f'\frac{\partial f'}{\partial \xi} - f''\frac{\partial f}{\partial \xi}\right) \tag{7}$$

$$\frac{\theta''}{Pr} + 3f\theta' = \xi\left(f'\frac{\partial \theta}{\partial \xi} - \theta'\frac{\partial f}{\partial \xi}\right) \tag{8}$$

along with the boundary conditions

$$f(\xi, 0) = -\frac{\xi}{4},$$

$$f'(\xi, 0) = \frac{1}{4}\frac{u_w x}{\nu}(Gr_x/4)^{-1/2} = \frac{1}{4}U_w\xi^2,$$

$$\theta(\xi, 0) = 1, \quad f'(\xi, \infty) = 0, \quad \theta(\xi, \infty) = 0. \tag{9}$$

In the above equations, the primes denote partial differentiation with respect to η, Pr is the Prandtl number, and the nonsimilarity parameter $\xi(x)$ is found to have the expression

$$\xi(x) = \frac{v_w x}{\nu}(Gr_x/4)^{-1/4}. \tag{10}$$

Surface injection corresponds to $\xi > 0$ and surface suction to $\xi < 0$. The dimensionless streamwise component of the mass transfer parameter, U_w, is defined as

$$U_w = \frac{u_w/v_w}{v_w x/\nu}. \tag{11}$$

For downstream vectoring $U_w > 0$ and for upstream vectoring $U_w < 0$. The expression for U_w in equation (11) is x-dependent; however, in the numerical solutions U_w is assumed constant. The interpretation of this assumption will be discussed later when numerical results are presented.

The physical quantities of interest are the velocity and temperature distributions, the heat transfer rate at the wall $q_w = -k(\partial T/\partial y)_{y=0}$ or the local Nusselt number $Nu_x = q_w x/[k(T_w - T_\infty)]$, and the wall shear stress $\tau_w = \mu(\partial u/\partial y)_{y=0}$. The streamwise velocity component u, the local Nusselt number Nu_x, and the local wall shear stress τ_w can be expressed by

$$u = 4(\nu/x)(Gr_x/4)^{1/2} f'(\xi, \eta) \tag{12}$$

$$Nu_x = -(Gr_x/4)^{1/4}\theta'(\xi, 0) \tag{13}$$

and

$$\tau_w = 4(\mu\nu/x^2)(Gr_x/4)^{3/4} f''(\xi, 0). \tag{14}$$

Horizontal plates

For this case, $\phi = \pi/2$, one introduces the following dimensionless variables:

$$\xi_1 = \xi_1(x), \quad \eta_1 = \frac{y}{x}(Gr_x/5)^{1/5} \tag{15}$$

along with the reduced stream function $f_1(\xi_1, \eta_1)$ and the dimensionless temperature function $\theta_1(\xi_1, \eta_1)$ defined, respectively, by

$$f_1(\xi_1, \eta_1) = \frac{\psi(x, y)}{5\nu(Gr_x/5)^{1/5}}, \quad \theta_1(\xi_1, \eta_1) = \frac{T - T_\infty}{T_w - T_\infty}. \tag{16}$$

The nonsimilar parameter $\xi_1(x)$ depends only on x. When $\xi_1(x) = 0$, the boundary layer is similar and η_1 becomes a true similarity variable. Substituting equations (15) and (16) into equations (2)–(4) with $\phi = \pi/2$, we obtain the following system of equations:

$$f_1''' + 3f_1 f_1'' - f_1'^2 + \frac{5}{2}\left[\eta_1\theta_1 + \int_{\eta_1}^{\infty}\theta_1\, d\eta_1 + \xi_1\int_{\eta_1}^{\infty}\frac{\partial\theta_1}{\partial\xi_1}d\eta_1\right] = 2\xi_1\left(f_1'\frac{\partial f_1'}{\partial\xi_1} - f_1''\frac{\partial f_1}{\partial\xi_1}\right) \tag{17}$$

$$\frac{\theta_1''}{Pr} + 3f_1\theta_1' = 2\xi_1\left(f_1'\frac{\partial\theta_1}{\partial\xi_1} - \theta_1'\frac{\partial f_1}{\partial\xi_1}\right) \tag{18}$$

with the boundary conditions

$$f_1(\xi_1, 0) = -\frac{\xi_1}{5},$$

$$f_1'(\xi_1, 0) = \frac{1}{5}\frac{u_w x}{\nu}(Gr_x/5)^{-2/5} = \frac{1}{5}U_w\xi_1^2,$$

$$\theta(\xi_1, 0) = 1, \quad f_1'(\xi_1, \infty) = 0, \quad \theta_1(\xi_1, \infty) = 0. \tag{19}$$

In the above equations, the primes now stand for partial differentiation with respect to η_1 and the nonsimilarity parameter $\xi_1(x)$ is found as

$$\xi_1(x) = \frac{v_w x}{\nu}(Gr_x/5)^{-1/5}. \tag{20}$$

Injection corresponds to $\xi_1 > 0$ and suction to $\xi_1 < 0$. The dimensionless streamwise component of the mass transfer parameter, U_w, is as defined by equation (11). The expressions for the streamwise velocity u, the local Nusselt number Nu_x, and the local wall shear stress τ_w for this case are given by

$$u = 5(\nu/x)(Gr_x/5)^{2/5} f_1'(\xi_1, \eta_1) \tag{21}$$

$$Nu_x = -(Gr_x/5)^{1/5}\theta_1'(\xi_1, 0) \tag{22}$$

and

$$\tau_w = 5(\mu\nu/x^2)(Gr_x/5)^{3/5} f_1''(\xi_1, 0). \tag{23}$$

It should be noted that when there is no mass transfer at the boundary, $\xi(x) = \xi_1(x) = 0$ and equations (7)–(9) and (17)–(19) reduce, respectively, to ordinary differential equations. If $\xi(x)$ or $\xi_1(x)$ is a constant, the system of equations (7)–(9) or (17)–(19) can again be reduced to a set of ordinary differential equations. By examining equation (10) or (20) one can see that for $\xi(x)$ or $\xi_1(x)$ constant, v_w must be a function of x and must vary with x as $v_w \propto x^{-1/4}$ or as $v_w \propto x^{-2/5}$. Since there are great difficulties in physically maintaining such a variable surface mass transfer, the present study is concerned only with constant surface mass transfer v_w and u_w, and thus the case of constant $\xi(x)$ or constant $\xi_1(x)$ is not considered.

METHOD OF SOLUTION

Equations (7)–(9) and (17)–(19) were solved by a finite difference method as described by Tien [8]. In this method, the partial differential equations are first reduced to a system of first-order equations which are then expressed in finite difference form and solved, along with the boundary conditions, by an iterative scheme. The set of coupled partial differential equations is first solved for $\xi = 0$ (or $\xi_1 = 0$), which pertains to a similar solution. For $\xi = 0$ (or $\xi_1 = 0$), a fourth-order Runge–Kutta integration scheme was employed, and the integration was performed from

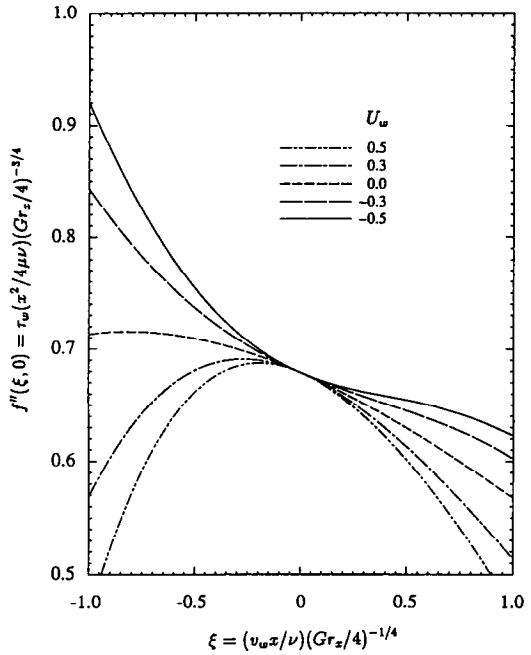

FIG. 1. Local wall shear stress results for vertical plates; $Pr = 0.7$.

$\eta = 0$ to $\eta = \eta_\infty$ (or $\eta_1 = 0$ to $\eta_1 = \eta_\infty$), where η_∞ is far enough from the wall to provide a finite approximation to $\eta = \infty$. In the present study, $\eta_\infty = 10$ was used in the numerical computations. The integration was performed with a step size $\Delta\eta$ (or $\Delta\eta_1$) of 0.02. Care was taken in choosing the proper step size $\Delta\eta$ (or $\Delta\eta_1$) for accurate converged solution and solutions were also obtained for $\Delta\eta$ (or $\Delta\eta_1$) of 0.01 and 0.04 to ensure the accuracy of the solution. With the solution for $\xi = 0$ (or $\xi_1 = 0$) and $0 \leqslant \eta \leqslant \eta_\infty$ (or $0 \leqslant \eta_1 \leqslant \eta_\infty$) available, the solution then proceeded to the next ξ (or ξ_1) location. The condition for $\xi > 0$ (or $\xi_1 > 0$) corresponds to a normal component of injection and that for $\xi < 0$ (or $\xi_1 < 0$) corresponds to a normal component of suction. This solution procedure was repeated for a succession of ξ (or ξ_1) values until converged solutions were obtained for the desired range of ξ (or ξ_1) values. The step size used for $\Delta\xi$ (or $\Delta\xi_1$) was 0.05. Numerical results were obtained for $Pr = 0.7$ over a range of values of the injection/suction parameter ξ (or ξ_1) and the streamwise mass transfer parameter U_w.

RESULTS AND DISCUSSION

Vertical plates

Numerical results for the local wall shear stress τ_w, expressed in terms of $\tau_w(x^2/4\mu\nu)(Gr_x/4)^{-3/4}$, and the local Nusselt number Nu_x, expressed in terms of $Nu_x(Gr_x/4)^{-1/4}$, as a function of $\xi = (v_w x/\nu) \times (Gr_x/4)^{-1/4}$, are shown, respectively, in Figs. 1 and 2 for values of U_w ranging from -0.5 to 0.5, with $Pr = 0.7$. The situation with $U_w > 0$ corresponds to downstream vectoring and that with $U_w < 0$ to upstream vectoring. In practical applications, Figs. 1 and 2 can be interpreted in different ways. If it is desired to study the effect of the horizontal component of mass transfer, u_w, on natural convection, we assign the values of v_w, Gr_x, and x. In doing so, we obtain a fixed value of ξ. A vertical line drawn through this value of ξ that intersects the curves for different U_w values represents changing values of u_w in the U_w expression. If it is desired to study the effect of the normal component of mass transfer, v_w, on natural convection, we assign the values of u_w, Gr_x, and x. A given value of ξ now represents a given value of v_w which can be used to fix U_w. Finally, if it is desired to study the effect of buoyancy on natural convection, we assign the values of u_w, v_w, and x. In doing so, U_w is fixed, and a change in the value of ξ now represents a change in the value of Gr_x.

It can be seen from Figs. 1 and 2 that for a given value of U_w, an increase in ξ in the positive sense (injection) results in a decrease in both the wall shear stress and the local Nusselt number (i.e. the surface heat transfer rate) for all the values of $-0.5 \leqslant U_w \leqslant 0.5$ that were computed. On the other hand, as ξ is increased in the negative sense (suction), the wall shear stress increases when $U_w < 0$, but it increases and then decreases when $U_w \geqslant 0$. Thus, for $U_w \geqslant 0$ there is a critical value of ξ for suction which results in the maximum wall shear stress. Increasing the suction beyond this point will result in a decrease in the wall shear stress. The heat transfer rate, however, increases with increasing values of $\xi < 0$ for both $U_w < 0$ and $U_w \geqslant 0$, and continues to increase

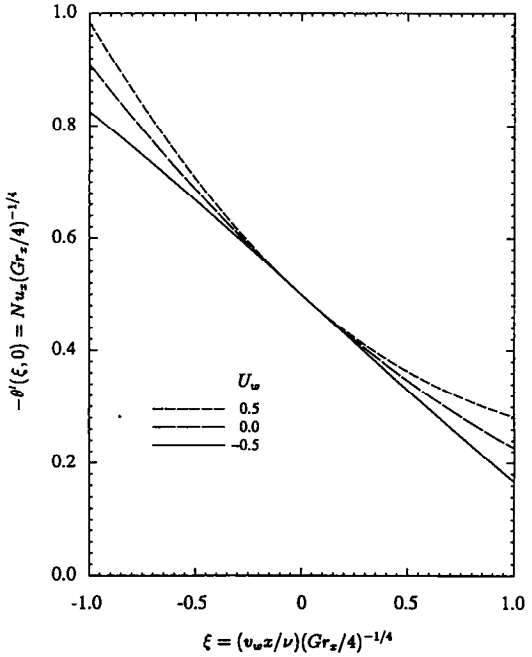

FIG. 2. Local Nusselt number results for vertical plates; $Pr = 0.7$.

even when the suction is increased past its critical value, beyond which the shear stress starts decreasing with ξ.

At first glance, there appears to be a contradiction in the trends between the local wall shear stress results and the local heat transfer results for the situation with $\xi < 0$ and $U_w \geqslant 0$. However, there is no contradiction and their behaviors can be explained by examining the velocity distributions $f'(\xi, \eta) = (1/4)(ux/\nu)(Gr_x/4)^{-1/2}$ shown in Figs. 3–5. It can be seen from the figures that the peak of the velocity distribution decreases as ξ increases in the negative sense. This indicates that the mass transfer normal to the wall in suction impedes the buoyancy force parallel to the wall. Thus, with increasing ξ value in the negative sense, the effective buoyancy force decreases and this results in a critical value of suction that will give rise to the maximum wall shear stress. Beyond this critical value the wall shear stress decreases, but the heat transfer rate increases. This is due to the fact that the peak of the velocity distribution and hence the entire flow boundary layer (see Fig. 5) shifts toward the wall beyond the critical value of suction. This causes a decrease in the thermal boundary layer thickness and an increase in the temperature gradient at the wall (see Fig. 8). Thus, for $\xi < 0$ and $U_w \geqslant 0$, even though the wall shear stress decreases as ξ becomes more negative, the heat transfer rate continues to increase. The temperature distributions $\theta(\xi, \eta) = [T(x, y) - T_\infty]/(T_w - T_\infty)$ for given values of U_w and ξ are shown in Figs. 6–8.

The local wall shear stress and the local Nusselt number as a function of U_w for a fixed ξ value are shown, respectively, in Figs. 9 and 10. It can be seen from the figures that for increasing U_w in the negative sense (increasing upstream vectoring), the local wall shear stress increases while the local surface heat transfer rate decreases. On the other hand, for increasing U_w in the positive sense (increasing downstream vectoring), the local wall shear stress decreases while the local surface heat transfer rate increases.

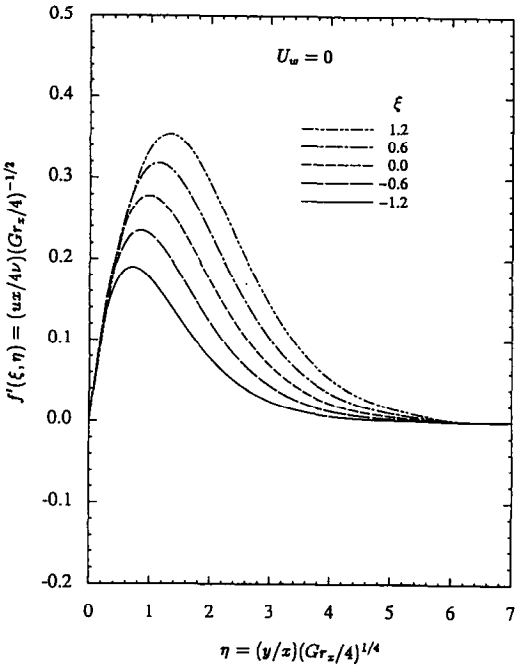

FIG. 4. Velocity profiles for vertical plates; $Pr = 0.7$, $U_w = 0$.

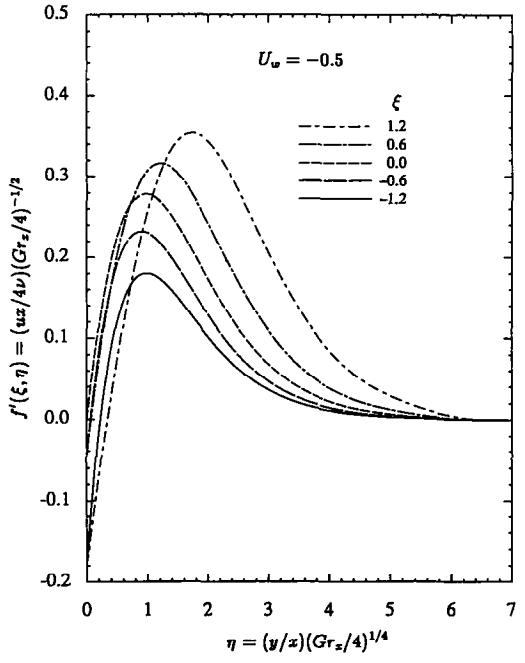

FIG. 3. Velocity profiles for vertical plates; $Pr = 0.7$, $U_w = -0.5$.

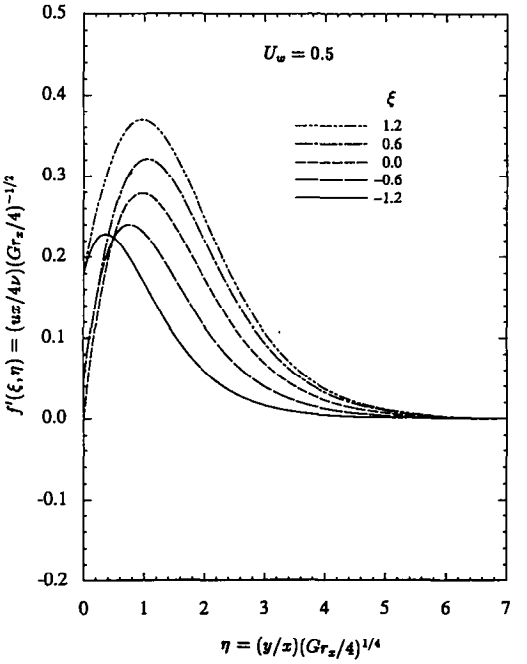

FIG. 5. Velocity profiles for vertical plates; $Pr = 0.7$, $U_w = 0.5$.

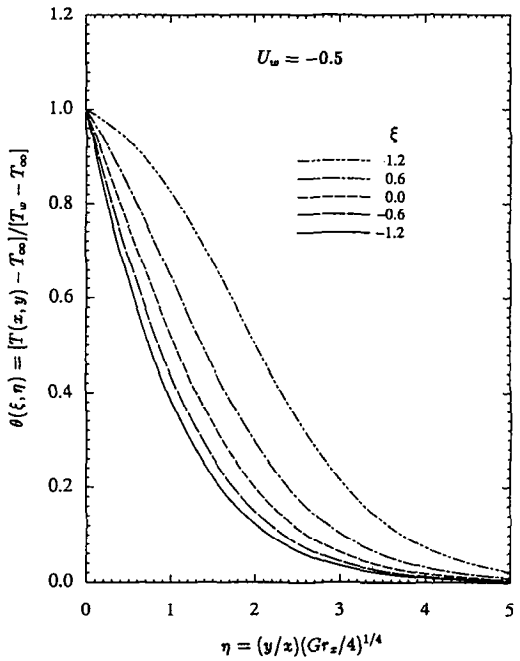

FIG. 6. Temperature profiles for vertical plates; $Pr = 0.7$, $U_w = -0.5$.

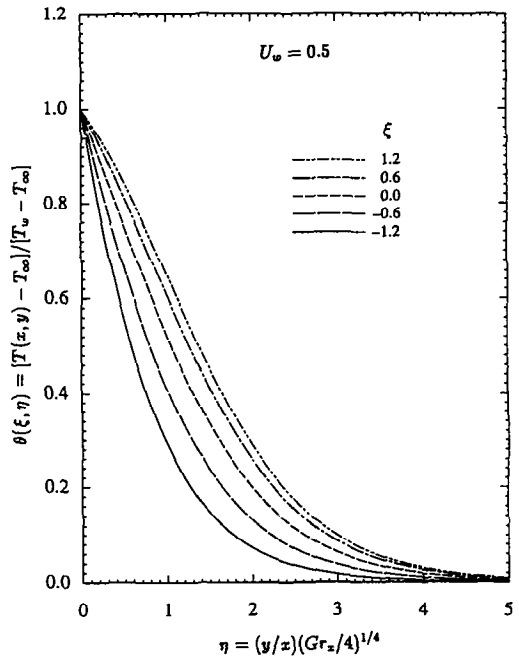

FIG. 8. Temperature profiles for vertical plates; $Pr = 0.7$, $U_w = 0.5$.

Horizontal plates

The local wall shear stress τ_w, expressed in terms of $\tau_w(x^2/5\mu\nu)(Gr_x/5)^{-3/5}$, and the local Nusselt number Nu_x, expressed in terms of $Nu_x(Gr_x/5)^{-1/5}$, as a function of $\xi_1 = (v_w x/\nu)(Gr_x/5)^{-1/5}$ for this case are shown, respectively, in Figs. 11 and 12 for values of U_w ranging from -0.5 to 0.5 with $Pr = 0.7$. For a given value of $U_w < 0$, it can be seen from these figures that an increase in ξ_1 in the positive sense (injection) results in an increase in the local wall shear stress and a decrease in the local Nusselt number (i.e. the local heat transfer rate at the wall) for all the values of $U_w < 0$ that were computed. On the other hand, for $U_w \geqslant 0$, an increase in ξ_1 in the positive sense gives rise to a decrease in both the local wall shear stress and the local surface heat transfer rate. Similarly, for a

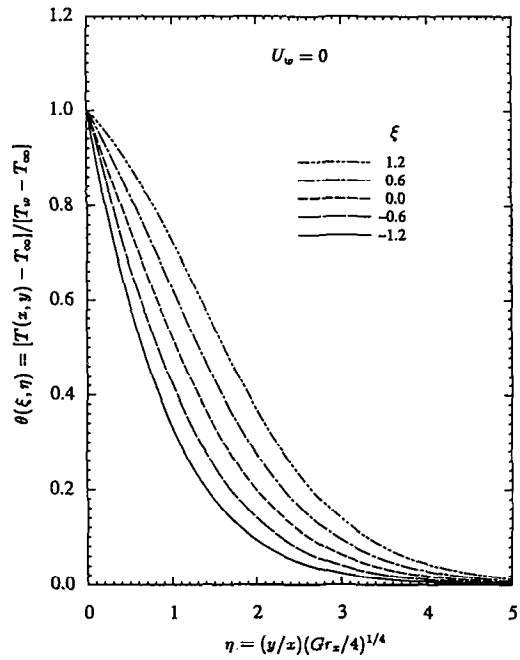

FIG. 7. Temperature profiles for vertical plates; $Pr = 0.7$, $U_w = 0$.

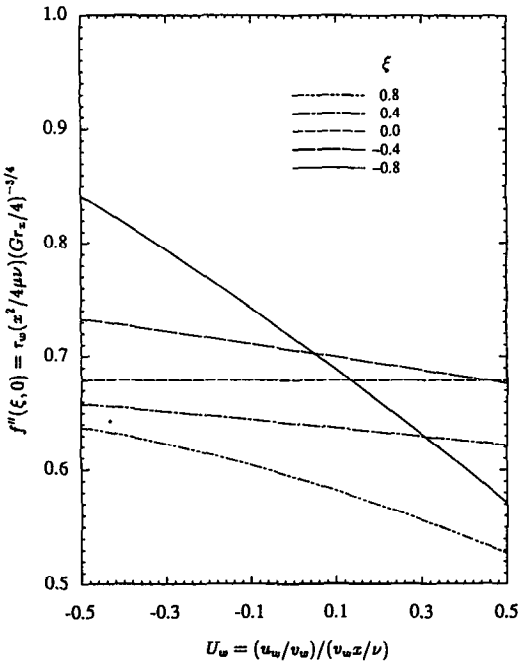

FIG. 9. Local wall shear stress vs U_w for vertical plates; $Pr = 0.7$.

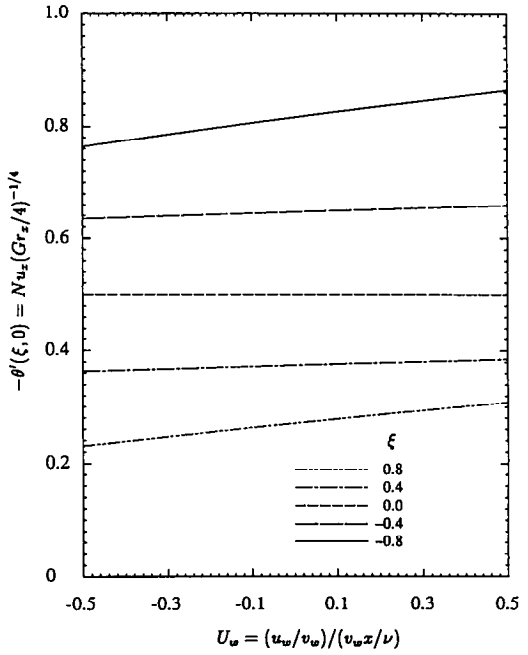

FIG. 10. Local Nusselt number vs U_w for vertical plates; $Pr = 0.7$.

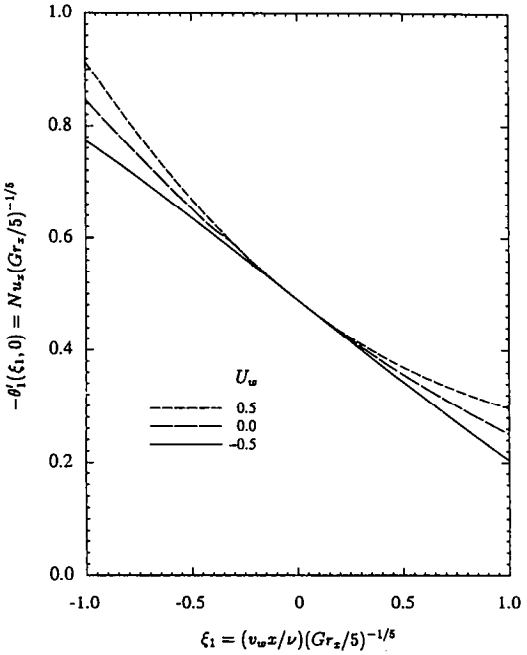

FIG. 12. Local Nusselt number results for horizontal plates; $Pr = 0.7$.

given value of $U_w < 0$, an increase in ξ_1 in the negative sense (suction) gives rise to an increase in both the local wall shear stress and the local surface heat transfer rate. However, for a given value of $U_w \geqslant 0$, an increase in ξ in the negative sense results in a decrease in the local wall shear stress and an increase in the local surface heat transfer rate. In practical applications, Figs. 11 and 12 can be interpreted in different ways, as was discussed earlier relative to Figs. 1 and 2 for the case of vertical plates.

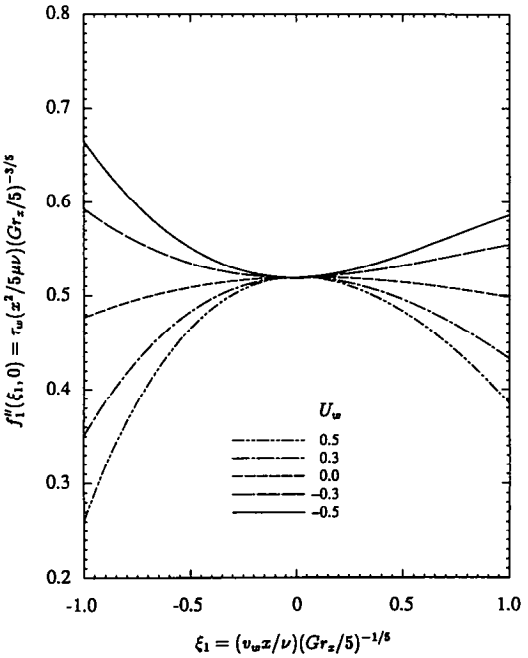

FIG. 11. Local wall shear stress results for horizontal plates; $Pr = 0.7$.

The behavior of the local wall shear stress and the local Nusselt number for horizontal plates with $U_w \geqslant 0$ can be explained from the velocity distributions in a manner similar to that discussed for the case of vertical plates. The velocity profiles for horizontal plates are similar to those of the vertical plates and are not shown to conserve space. It suffices to mention that the peak of the velocity distribution decreases as ξ_1 increases in the negative sense (suction). This implies that increasing suction normal to the wall decreases the effective buoyancy force and hence the wall shear stress when $U_w \geqslant 0$. However, the surface heat transfer rate increases. This is because the peak of the velocity distribution shifts toward the wall as ξ_1 becomes more negative and as U_w increases from a negative to a positive value, which causes the thinning of the thermal boundary layer and an increase in the temperature gradient at the wall. On the other hand, an increase of ξ_1 in the positive sense (injection) gives rise to an increase in the peak velocity, which shifts away from the wall. Thus, for $\xi > 0$ and $U_w \geqslant 0$, as ξ increases the local wall shear stress decreases, and the local heat transfer rate also decreases as a result of the decrease in the wall temperature gradient. The temperature distributions $\theta_1(\xi_1, \eta_1) = [T(x,y) - T_\infty]/(T_w - T_\infty)$ for given values of U_w and ξ_1 are similar to those of the vertical plates and are not shown.

Figures 13 and 14 illustrate the local wall shear stress and the local Nusselt number (i.e. the local surface heat transfer rate) as a function of U_w for a fixed ξ value. As in the case of vertical plates, it is seen

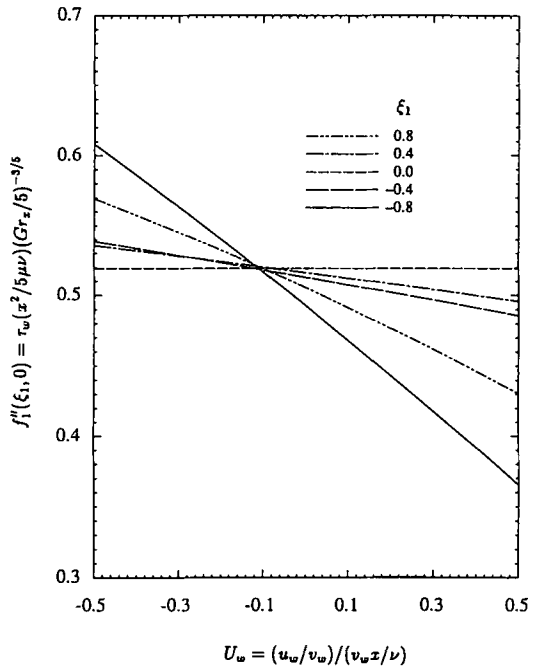

FIG. 13. Local wall shear stress vs U_w for horizontal plates; $Pr = 0.7$.

that for increasing U_w in the negative sense (increasing upstream vectoring), the local wall shear stress increases while the local surface heat transfer rate decreases. For increasing U_w in the positive sense (increasing downstream vectoring), the local wall shear stress decreases while the local surface heat transfer rate increases.

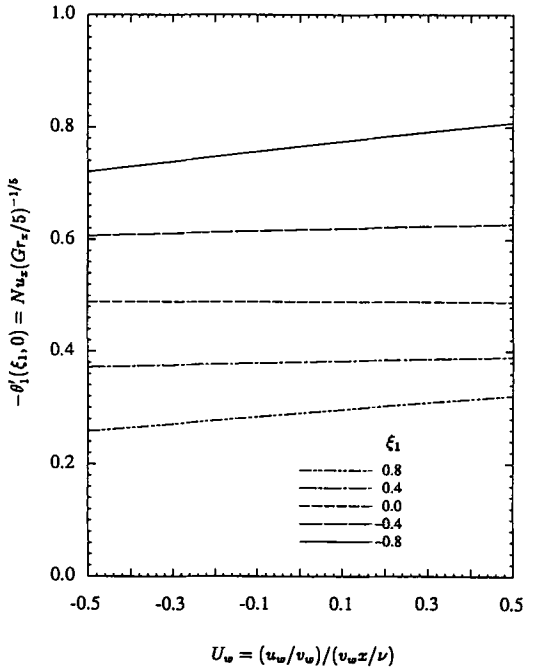

FIG. 14. Local Nusselt number vs U_w for horizontal plates; $Pr = 0.7$.

A thorough comparison of the present results cannot be made with existing work, because no numerical solutions or experimental data for natural convection on vertical and horizontal plates with uniform vectored surface mass transfer are available. The results from the present study for the case of vertical plates with normal surface mass transfer without the vectoring (i.e. no streamwise component of mass transfer) compare very well with those of Minkowycz and Sparrow [9]. Their solution was obtained using the local nonsimilarity method truncated at the second level.

CONCLUSION

In this paper, natural convection in laminar boundary layer flows over isothermal vertical and horizontal flat plates under uniform vectored surface mass transfer has been studied analytically. The motivation is to determine the effect of buoyancy and mass transfer on the flow and heat transfer characteristics of the boundary layer by changing the values of v_w (the normal component of the uniform mass transfer), u_w (the streamwise component of the uniform mass transfer), and Gr_x (the local Grashof number).

For the case of vertical plates, the local wall shear stress and the local surface heat transfer rate decrease with increasing ξ in the positive sense (normal injection) for given values of u_w and Gr_x. Increasing ξ in the negative sense (normal suction) causes an increase in the local surface heat transfer rate. For downstream vectoring ($U_w > 0$), the local wall shear stress increases as suction increases until a critical value of ξ is reached. Increasing ξ beyond this critical value results in a decreasing local wall shear stress. For upstream vectoring ($U_w < 0$), both the local wall shear stress and the local surface heat transfer rate increase with increasing ξ in the negative sense.

For horizontal plates it has been found that the local wall shear stress increases and the local wall heat transfer rate decreases with increasing ξ_1 in the positive sense (normal injection) for $U_w < 0$ (upstream vectoring). For $U_w > 0$ (downstream vectoring), increasing ξ_1 in the positive sense results in a decrease in both the local wall shear stress and the local surface heat transfer rate. Increasing ξ_1 in the negative sense (normal suction) gives rise to an increase in both the local surface heat transfer rate and the local wall shear stress for $U_w < 0$, but a decrease in the local wall shear stress and an increase in the local surface heat transfer rate for $U_w > 0$.

For both vertical and horizontal plates, with a given value of ξ, positive or negative, increasing U_w in the positive sense (downstream vectoring) results in a decrease in the local wall shear stress and an increase in the local surface heat transfer rate. On the other hand, increasing U_w in the negative sense (upstream vectoring) results in an increase in the local wall shear

stress and a decrease in the local surface heat transfer rate. An increase in the buoyancy intensity (i.e. the Grashof number Gr_x) for given u_w and v_w gives rise to an increase in the local wall shear stress and the local surface heat transfer rate. A decrease in Gr_x for given u_w and v_w, on the other hand, results in a decrease in the two quantities.

Acknowledgement—The authors would like to thank Mr Bin Hong for drawing the figures presented in this paper.

REFERENCES

1. T. F. Swean and G. R. Inger, Vectored injection and suction in laminar boundary layers with heat transfer, *AIAA J.* **13,** 616–622 (1975).
2. T. S. Chen and E. M: Sparrow, Flow and heat transfer over a flat plate with uniformly distributed, vectored surface mass transfer, *J. Heat Transfer* **98,** 674–676 (1976).
3. S. Tsuruno and I. Iguchi, Prediction of combined free and forced convective heat transfer along a vertical plate with uniform blowing, *J. Heat Transfer* **102,** 168–170 (1980).
4. A. Yucel, Mixed convection on a horizontal surface with injection or suction, *J. Thermophys. Heat Transfer* **3,** 476–479 (1989).
5. J. Dey, Mixed convection flow over a semi-infinite horizontal plate with vectored mass transfer, *J. Heat Transfer* **104,** 558–560 (1982).
6. P. G. Parikh, R. J. Moffat, W. M. Kays and D. Bershader, Free convection over a vertical porous plate with transpiration, *Int. J. Heat Mass Transfer* **17,** 1465–1474 (1974).
7. T. S. Chen, H. C. Tien and B. F. Armaly, Natural convection on horizontal, inclined, and vertical plates with variable surface temperature or heat flux, *Int. J. Heat Mass Transfer* **29,** 1465–1478 (1986).
8. H. C. Tien, Heat transfer and instability of natural convection flow on inclined flat plates, Master's Thesis, Department of Mechanical and Aerospace Engineering, University of Missouri–Rolla (1985).
9. W. J. Minkowycz and E. M. Sparrow, Numerical solution scheme for local nonsimilarity boundary layer analysis, *Numer. Heat Transfer* **1,** 69–85 (1978).